

114521

131956

P.26

NASA Technical Memorandum 105903

Structural Optimization of Thin Shells Using Finite Element Method

Pascal K. Gotsis
*Lewis Research Center
Cleveland, Ohio*

October 1992

(NASA-TM-105903) STRUCTURAL
OPTIMIZATION OF THIN SHELLS USING
FINITE ELEMENT METHOD (NASA) 26 p

N93-13157

Unclass

G3/39 0131956



4821115



STRUCTURAL OPTIMIZATION OF THIN SHELLS USING FINITE ELEMENT METHOD

Pascal K. Gotsis
National Aeronautics and Space Administration
Lewis Research Center
Cleveland, Ohio 44135

ABSTRACT

The objective of the present work was the structural optimization of thin shell structures that are subjected to stress and displacement constraints. In order to accomplish this, the structural optimization computer program DESAP1 was modified and improved. In the static analysis part of the DESAP1 computer program the torsional spring elements, which are used to analyze thin, shallow shell structures, were eliminated by modifying the membrane stiffness matrix of the triangular elements in the local coordinate system and adding a fictitious rotational stiffness matrix. This simplified the DESAP1 program input, improved the accuracy of the analysis, and saved computation time. In the optimization part of the DESAP1 program the stress ratio formula, which redesigns the thickness of each finite element of the structure, was solved by an analytical method. This scheme replaced the iterative solution that was previously used in the DESAP1 program, thus increasing the accuracy and speed of the design. The modified program was used to design a thin, cylindrical shell structure with optimum weight, and the results are reported in this paper.

1. INTRODUCTION

1.1 General

In the past, discrete optimality criteria have been derived for a number of design conditions including strength, static stiffness, dynamic stiffness, static stability, and aeroelastic constraints. The computer programs DESAP [1], DESAP2 [2], and FASTOP [3], as well as OPSTAT, OPTCOMP, OPTIM, ASOP [4], and others, use the discrete optimality criteria approaches as a basis for structural optimization. These programs are based on the finite element method of analysis and can optimize isotropic, anisotropic, and layered composite structures. The codes can handle over 1000 design variables and a comparable number of analysis variables, which are the degrees of freedom.

This paper examines the structural optimization of thin, shallow shells by using the DESAP1 structural optimization program. DESAP1 was developed to design structures with linear elastic material behavior. The total weight of the structure is minimized by computing the element sizes, that is, the cross-sectional areas for trusses and beams and the thicknesses for plates and shells, under certain constraints. The static analysis of the design is computed by using the finite element method. For purpose of analysis the SAPIV finite element program [5] was modified for use in the DESAP1 computer program. The synthesis algorithm of DESAP1 consists of iterative processes. Each iterative process comprises three steps: (1) static analysis of the current design, (2) comparison and evaluation of the results of the static analysis, and (3) redesign of the structure by using information from the previous two steps.

Two kinds of constraints are used in DESAP1: primary constraints and secondary constraints. The primary constraints are displacements and stresses with upper limits. The stress constraints are failure criteria, or local instability criteria, or both. If stress constraints are used in the redesign of the structure, the stress ratio method [1, 6, 7] is applied to drive the

final design to the fully stressed design. In the fully stressed design each element is assumed to reach the allowable stress under at least one load condition. The fully stressed design always coincides with the minimum-weight design for statically determined structures, but the design need not be fully stressed at optimum for statically indeterminate structures, in general. For displacement constraints the redesign procedure [6] is based on an optimality criteria method, and the element sizes (thicknesses) are obtained for the optimum weight design.

The secondary constraints consist of the minimum allowable element sizes and the size proportional constraints, whereas the element sizes have a prescribed ratio. In the DESAP1 program it is assumed that the static loading is independent of the element sizes. Also, during the design procedure the layout of the structure is not changed.

This study involved the following steps:

(1) In the static analysis part of the DESAP1 program the torsional spring elements, which are used to analyze thin, shallow shell structures, were eliminated by modifying the membrane stiffness matrix of the triangular elements in the local coordinate system and adding a fictitious rotational stiffness matrix as suggested by Zienkiewicz [8, 9].

(2) In the optimization part of the DESAP1 computer program the iterative solution of a fourth-order equation, which redesigns the thickness of each finite element of the structure, was replaced by an analytical solution.

(3) A thin shell structure was designed to minimize its weight and was subjected to stress and displacement constraints.

1.2 Element properties

The weight W_i of an element i can be written as

$$W_i = p_i t_i \quad i = 1, \dots, I$$

where p_i is the unit weight and t_i is the size (thickness) of the element i . Because it is not desirable to have each t_i as an independent variable, the form

$$t_i = n_i D_m$$

is introduced for $i = 1, \dots, I$ and $m = 1, \dots, M < I$, where D_m are independent variables and n_i is the design variable fraction of the element. For each element, n_i and m must be defined [1].

The stiffness matrix $[K_i]$ of element i can be written as

$$[K_i] = [K_i^{(1)}]t_i + [K_i^{(2)}]t_i^{n_i}$$

where $[K_i^{(1)}]$ is the unit stiffness matrix due to the action of the direct stresses, $[K_i^{(2)}]$ is the unit stiffness matrix due to the bending or torsion, and n_i is the inertia exponent, which is determined by the relationship between the size and moment of inertia of the element as follows:

$$I_i = J_i t_i^{n_i}$$

where J_i is the unit moment of inertia.

The vector of the internal forces $\{N_i\}$ of node i is computed from the previously computed element nodal displacements $\{u_i\}$ as follows:

$$\{N_i\} = [S_i]\{u_i\} + \{T_i\}$$

where $[S_i]$ is the recovery matrix and $\{T_i\}$ is the force vector [1].

1.3 Stress-ratio formula

If stress constraints are imposed in the DESAP1 program, the stress ratio method is used. In order to obtain the redesign stress ratio formula, the Von Mises yield criterion is applied at each element of the plate or shell structure.

First, the assumption is made that a single load condition is imposed in the structure. The yield criterion f for an element i has the general form:

$$f(\{N_i\}, \{N_i^*\}, t) = 1 \quad (1)$$

where $\{N_i\}$ is the vector of the internal forces on the nodes of an element i due to a single load condition; $\{N_i^*\}$ is the vector of the allowable forces; and t is the thickness of an element i of the plate or shell structure.

If the improved design is to be fully stressed and $\{N_i'\}$ and t' are the improved values, the following form must be satisfied:

$$f(\{N_i'\}, \{N_i^*\}, t') = 1 \quad (2)$$

If $\{N_i'\}$ is known, the improved value of the thickness t' is calculated from Eq. (2). The calculation of $\{N_i'\}$ is obtained by inverting the structural stiffness matrix. In the DESAP1 program this inversion is impractical for large structures because the banded form of the structural stiffness matrix is lost after its inversion. For this reason it is assumed that the nodal forces $\{N_i'\} = \{N_i\}$ do not change. Substituting the values of $\{N_i'\}$ into Eq. (2) gives the following equation:

$$f(\{N_i\}, \{N_i^*\}, t') = 1 \quad (3)$$

The solution procedure consists of solving Eq. (3) for t' load conditions at a time and then choosing the largest value for the improved thickness. This procedure is the stress ratio method of redesign as it is used in the DESAP1 program. Equation (3) is an approximation and must be applied iteratively, updating $\{N_i\}$ each time, before a fully stressed design is obtained.

In order to check the design process, the following two controls were established:

(1) The design is critical if

$$(1 - d) \leq R_{\max} \leq (1 + d)$$

where d is a small parameter described by the user of the program that expresses the desired width of the critical design band; R_{\max} is equal to $\max(D'_m/D_m)$, where D_m and D'_m are

the previous and the new values, respectively, and D'_m is the largest value of the following two equations:

$$D'_m = t'/n_i$$

where n_i is a parameter described by the user for an element i , or

$$D'_m = D_m^*$$

where D_m^* is the prescribed lower thickness of the secondary constraints. When equal or proportional size constraints are used, D'_m is defined by choosing the largest value of the following two equations:

$$D'_m = \max (t'/n_i)$$

or

$$D'_m = D_m^*$$

(2) The design is fully stressed if it satisfies the following two conditions simultaneously:

$$(1 - d) \leq R_{\max} \leq (1 + d) \quad (\text{critical design})$$

and

$$(1 - d) \leq R_{\min} \leq (1 + d)$$

where R_{\min} is equal to $\min (D'_m = D_m)$.

1.4 Hencky–Von Mises failure criterion

In this study the plate or shell structure was assumed to consist of material that is isotropic and homogeneous. The Hencky–Von Mises failure criterion was used to obtain the redesign stress ratio formula. The failure function f of Eq. (1) takes the following form:

$$f = (S_x/S_x^*)^2 + (S_y/S_y^*)^2 - S_x S_y / S_x^* S_y^* + (S_{xy}/S_{xy}^*)^2 = 1 \quad (4)$$

where S_x and S_y are the normal stresses at a point in the element, S_{xy} is the shear stress at a point in the element, and S_x^* , S_y^* , and S_{xy}^* are the allowable normal and shear stresses.

The basic assumption was that the resulting internal forces remain unchanged during the redesign:

$$N'_x = N_x$$

$$N'_y = N_y$$

$$N'_{xy} = N_{xy}$$

$$M'_x = M_x$$

$$M'_y = M_y$$

$$M'_{xy} = M_{xy}$$

where N' and M' are the values of the improved design and N and M are the values of the previous design.

The internal stresses that are developed in the shell under the external static load consist of the membrane components and the bending components. The membrane stresses S'_x , S'_y , and S'_{xy} at a point are given by

$$S'_x = N_x/t' \quad (5a)$$

$$S'_y = N_y/t' \quad (5b)$$

$$S'_{xy} = N_{xy}/t' \quad (5c)$$

where S' is the value of the improved design and t' is the value of the improved thickness of an element of the shell structure. The allowable membrane stresses are

$$S_x^* = N_x^*/t$$

$$S_y^* = N_y^*/t$$

$$S_{xy}^* = N_{xy}^*/t$$

The bending stresses S'_x , S'_y , and S'_{xy} at a point are given by [10]

$$S'_x = \pm 6M_x/t'^2 \quad (6a)$$

$$S'_y = \pm 6M_y/t'^2 \quad (6b)$$

$$S'_{xy} = \pm 6M_{xy}/t'^2 \quad (6c)$$

The allowable bending stresses are

$$S_x^* = 6M_x^*/t^2$$

$$S_y^* = 6M_y^*/t^2$$

$$S_{xy}^* = 6M_{xy}^*/t^2$$

Therefore, in a shell structure the stresses at a point are given by the following forms:

$$(S'_x/S_x^*) = (S'_x/S_x^*)_{\text{membrane}} + (S'_x/S_x^*)_{\text{bending}} \quad (7a)$$

$$(S'_y/S_y^*) = (S'_y/S_y^*)_{\text{membrane}} + (S'_y/S_y^*)_{\text{bending}} \quad (7b)$$

$$(S'_{xy}/S_{xy}^*) = (S'_{xy}/S_{xy}^*)_{\text{membrane}} + (S'_{xy}/S_{xy}^*)_{\text{bending}} \quad (7c)$$

From Eq. (7a)

$$(S'_x/S_x^*) = (N_x/N_x^*) (t/t') \pm (M_x/M_x^*)(t/t')^2 \quad (8a)$$

Similarly,

$$(S'_y/S_y^*) = (N_y/N_y^*) (t/t') \pm (M_y/M_y^*)(t/t')^2 \quad (8b)$$

and

$$(S'_{xy}/S_{xy}^*) = (N_{xy}/N_{xy}^*) (t/t') \pm (M_{xy}/M_{xy}^*)(t/t')^2 \quad (8c)$$

Multiplying Eqs. (8a) and (8b) gives

$$\begin{aligned} (S'_x/S_y^*)/(S_x^*/S'_y) &= [(N_x/N_x^*)(t/t') \pm (M_x/M_x^*)(t/t')^2] \\ &\times [(N_y/N_y^*)(t/t') \pm (M_y/M_y^*)(t/t')^2] \end{aligned} \quad (8d)$$

Substituting the values S'_x/S_x^* , S'_y/S_y^* , and S'_{xy}/S_{xy}^* from Eqs. (8) into Eq. (4) yields the following equation:

$$\begin{aligned}
& [(N_x/N_x^*)(t/t') \pm (M_x/M_x^*)(t/t')^2]^2 + [(N_y/N_y^*)(t/t') \pm (M_y/M_y^*)(t/t')^2]^2 \\
& + [(N_{xy}/N_{xy}^*)(t/t') \pm (M_{xy}/M_{xy}^*)(t/t')^2]^2 - [(N_x/N_x^*)(t/t') \pm (M_x/M_x^*)(t/t')^2] \\
& \quad \times [(N_y/N_y^*)(t/t') \pm (M_y/M_y^*)(t/t')^2] = 1
\end{aligned}$$

Simplifying this equation gives

$$(t'/t)^4 - C_{xx}(t'/t)^2 \mp C_x(t'/t) - C = 0 \quad (9)$$

where the minus sign preceding C_x is applicable to the upper surface of the plate or shell, and the plus sign, to the lower surface. In Eq. (9) the following notation was used:

$$C_{xx} = (N_x/N_x^*)^2 + (N_y/N_y^*)^2 + (N_{xy}/N_{xy}^*)^2 - N_x N_y / N_x^* N_y^* \quad (10a)$$

$$\begin{aligned}
C_x = 2[(N_x/N_x^*)(M_x/M_x^*) + (N_y/N_y^*)(M_y/M_y^*) + (N_x^*/N_y^*)(M_{xy}/M_{xy}^*)] \\
- [(N_x/N_x^*)(M_y/M_y^*) + (N_y/N_y^*)(M_{xy}/M_{xy}^*)]
\end{aligned} \quad (10b)$$

and

$$C = (M_x/M_x^*)^2 + (M_y/M_y^*)^2 + (M_{xy}/M_{xy}^*)^2 - (M_x/M_x^*)(M_y/M_y^*) \quad (10c)$$

Further investigation into Eqs. (10a) and (10c) (see Appendix) gives $C_{xx} \geq 0$ and $C \geq 0$.

These inequalities were used to find the positive and real solution of the quartic Eq. (9).

In order to solve the quartic equation

$$X^4 - C_{xx}X^2 \mp C_xX - C = 0 \quad (11)$$

where $X = t'/t$, it was reduced to the resolvent cubic equation [11]. The resolvent cubic equation of the quartic is

$$y^3 + Ay^2 + By + D = 0 \quad (12)$$

where $A = -C_{xx}$, $B = 4C$, and $D = -C_x^2 - 4C_{xx}C$. The analytical solution of the roots of the cubic Eq. (12) according to Cardan's method is described by Borofsky [12]. By the analytical solution of the quartic equation, a much greater accuracy and computational efficiency was achieved than when an iteration method was used to obtain the solution.

2. SHELL STRUCTURES

The original DESAP1 computer program uses torsional spring elements, which are springs that are defined as normal to the flat shell surface, to eliminate the singularity of the total stiffness matrix in the global coordinate system. Because it is time consuming to define the normal direction at each point on the shell structure surface, the DESAP1 subroutines were modified so that thin shells could be designed without using the torsional spring elements. In order to explain the procedure that was followed, shell structures and finite element theory are reviewed briefly.

The classical theory of shell structures is discussed by Flugge [13]. When applying the finite element method to shell problems, it is assumed that the behavior of a continuously curved surface can be represented by the behavior of a surface that is built up with small flat elements. In any shell structure the elements generally will be subjected to both bending and in-plane forces [14]. For example, consider typical triangular flat elements that are subjected simultaneously to in-plane and bending actions (Figs. 1 and 2). In Fig. 1, u_n and v_n ($n = i, j, k$) are the nodal displacements, and U_n and V_n are the corresponding nodal forces. In Fig. 2, W_n , θ_{xn} , and θ_{yn} ($n = i, j, k$) are the nodal displacements, and W_n , M_{xn} , and M_{yn} are the corresponding nodal forces. Taking first the in-plane (plane stress) action, the state of the strain is uniquely described in terms of the u_i and v_i displacement of each typical node i in the x' and y' local coordinate directions, respectively. The minimization of the total potential

energy led to the stiffness matrices described by Zienkiewicz [8], which relate nodal forces F^P to displacement parameters

$$F^P = K^P d^P$$

For a triangular element K^P is a 6-by-6 matrix [7].

Similarly, when bending is considered, the state of strain is given uniquely by the nodal displacement w_i and the two rotations θ_{xi} and θ_{yi} at each node i (Fig. 3). The corresponding nodal forces are given by

$$F^b = K^b d^b$$

For a triangular element K^b is a 9-by-9 matrix [7].

Before combining the in-plane and bending stiffnesses note (1) that the displacements prescribed for in-plane forces do not affect the bending deformations and vice versa and (2) that rotation θ_{zi} about the z' axis is not involved in the deformations in either node. Combining the membrane and bending actions and introducing θ_{zi} and its associate couple M_{zi} gives for an element node i the following nodal displacements d_i and nodal forces F_i :

$$d_i = \left[u_i \ v_i \ w_i \ \theta_{xi} \ \theta_{yi} \ \theta_{zi} \right]^T$$

and

$$F_i = \left[U_i \ V_i \ W_i \ M_{xi} \ M_{yi} \ M_{zi} \right]^T$$

For an element

$$F = kd \tag{13}$$

where for a triangular element containing nodes i, j , and k the element force and displacement vectors are

$$F = \left[F_i \ F_j \ F_k \right]^T$$

$$d = \left[d_i \ d_j \ d_k \right]$$

and the element stiffness matrix in the local coordinates is

$$\mathbf{K} = \mathbf{K}^p + \mathbf{K}^b \quad (14)$$

The total stiffness matrix \mathbf{K} is an 18-by-18 matrix and is illustrated in Fig. 3.

2.1 Replacement of torsional spring elements

In a shallow shell structure, if all the elements meeting at a node i are coplanar, numerical problems due to the singularity of the stiffness matrix arise in the DESAP1 program. Because it was assumed that the moment M_{zi} and the stiffness are zero in the θ_{zi} direction in the local system (Fig. 1), the sixth row and column of each submatrix \mathbf{K}_{rs} of the total stiffness matrix contain zeroes [7]. If the set of all equilibrium equations is considered at the point i , in the local system, six equations result, of which the sixth equation is

$$M_{zi} = O_{ui} + O_{vi} + O_{wi} + O\theta_{xi} + O\theta_{yi} + O\theta_{zi} \quad (15)$$

or $0 = 0$. The difficulty persists when the six equilibrium equations at the point i are transformed to global coordinates. Because these equations will still have a singular matrix, a solution cannot be obtained [8, 9, 15]. The following three techniques for eliminating the singularity of the stiffness matrix have been used in existing literature:

(1) References 8,15, and 16 eliminate the sixth row and column from the stiffness matrix to obtain a nonsingular 5-by-5 stiffness matrix. However, it is impractical to apply this technique to DESAP1 because programming difficulties are encountered that would require an extensive revision of the DESAP1 source program.

(2) The DESAP1 and SAPIV computer programs use the torsional spring elements to eliminate the singularity of the stiffness matrix. The spring element has a torsional stiffness that is normal to the shell surface (Fig. 4). Two methods are used to specify the direction of the spring elements in DESAP1 (Figs. 5 and 6). In the first method the direction is determined by

the structural node N and a second node I (Fig. 5). Node I may be a structural node or a special node. In the latter case the degrees of freedom of node I should be suppressed on the node. In the second method the direction of the element is taken as perpendicular to the lines IJ and KL (Fig. 6). The points I, J, K, and L may be structural nodes or special points (with suppressed degrees of freedom). The torsional spring elements give rise to additional terms along the diagonal of the element stiffness matrix \mathbf{K} [7]. These new terms have values that are equal to the rotational stiffness of the spring. Transforming the matrix \mathbf{K} of each element to the global system and adding all the matrices give a nonsingular stiffness matrix of the structure.

Although the use of torsional spring elements in eliminating the singularity is feasible, it is both difficult and time consuming to find the directions that are normal to the shell structure at the nodal points in order to define the new nodes and the torsional stiffnesses associated with them. Therefore, discovering a simpler way to overcome the use of boundary elements would save time and make the program easier to use.

(3) References 8, 9, and 17 eliminate the singularity of the stiffness matrix by adding a fictitious rotational stiffness matrix in the membrane stiffness matrix \mathbf{K}^P . Here it is assumed that a nodal rotation θ_{zi} about the z' local axis of any one triangular element node is responsible only for the development of resisting couples M_{zi} , M_{zj} , and M_{zk} at the three element nodes and does not produce any other reactions. In order to ensure static equilibrium, the sum of the couples M_{zi} , M_{zj} , and M_{zk} is always taken to be zero. Zienkiewicz et al. [8, 9] determined that satisfactory results are obtained if these couples are proportional to the modulus of elasticity E and the volume At of the triangular element, where A is the area and t is the thickness of the element. They suggested the following moment-rotation relationship:

$$\begin{Bmatrix} M_{zi} \\ M_{zj} \\ M_{zk} \end{Bmatrix} = aEAt \begin{bmatrix} 1 & -0.5 & -0.5 \\ -0.5 & 1 & -0.5 \\ -0.5 & -0.5 & 1 \end{bmatrix} \cdot \begin{Bmatrix} \theta_{zi} \\ \theta_{zj} \\ \theta_{zk} \end{Bmatrix} \quad (16)$$

where a is an undetermined coefficient. A realistic value of a was estimated to be approximately 0.03 [9, 17]. A displacement error of about 10 percent is caused by introducing a value as large as 1.0. The displacements for very small values of a are nearly exact. However, for practical purposes, extremely small values of a are possible only when a large computational precision is available. In the present research a value of $a = 0.03$ was used so that Eq. (16) can be written as

$$\begin{Bmatrix} M_{zi} \\ M_{zj} \\ M_{zk} \end{Bmatrix} = \begin{bmatrix} B & -B/2 & -B/2 \\ -B/2 & B & -B/2 \\ -B/2 & -B/2 & B \end{bmatrix} \cdot \begin{Bmatrix} \theta_{zi} \\ \theta_{zj} \\ \theta_{zk} \end{Bmatrix} \quad (17)$$

where $B = 0.03EAt$. Adding the stiffness coefficients B and $-B/2$ of Eq. (17) in the appropriate positions in the membrane stiffness matrix \mathbf{K}^P in the local system yields a new membrane stiffness matrix of the element [7]. The combination of the updated membrane stiffness matrix and the bending stiffness matrix gives the total stiffness matrix in the local system for a triangular element i, j, k (Fig. 3). (In Fig. 3, $C = B/2$.) Transforming the total stiffness matrix from the local to the global system of each element and adding them gives a nonsingular structural stiffness matrix. This procedure eliminates the singularity of the structural stiffness matrix in the global system for shallow shell structures in the DESAP1 computer program.

3. EXAMPLE PROBLEM: THIN SHELL STRUCTURE

Consider a thin, cylindrical shell structure with an angle of 10° (Figs. 7 and 8) that is subjected to a concentrated load of 128 kips at the center. The shell, 36 ft long and 30 ft wide, is simply supported at the two opposite edges and is free at the other two edges. The material behavior of the structure is linear elastic, isotropic, and homogeneous. The design of the shell structure was obtained by the modified DESAP1 program. Because of the symmetry of the shell structure, only one-fourth of the shell (Fig. 9) is required to employ the finite element method.

Young's modulus of elasticity of the material is 4.38×10^8 lb/ft², the specific weight is 360 lb/ft³, and the Poisson's ratio is 0.3. The concentrated load on the quarter shell structure is 32 kips. The design commenced with a uniform thickness t for all the elements equal to 1.14 ft. The minimum size constraint for all the element thicknesses was 0.1 ft. All the plate elements were sized independently.

Both displacement and stress constraints were used. Only the displacement constraints were used first to allow for the thickness of the element to converge faster; they were applied at the center of the shell structure. The magnitude of the displacement constraint is 0.055 ft in the z direction. The stress constraints are added later, and the magnitude of the allowable stress in tension S_t^* is 25 000 lb/ft². The allowable stress in compression S_c^* is also 25 000 lb/ft².

The design is acceptable if it meets two criteria [1, 6]. The first criterion is satisfied (1) if the design is fully stressed, as discussed earlier, and (2) if the displacement constraints are not violated; that is, $Q_{\max} \leq (1 + d)$, where Q_{\max} is the displacement ratio, which is defined as the displacement of a node over the maximum allowable displacement at the node, and d is a small parameter described previously. The second criterion is satisfied (1) if the design is displacement critical (i.e., $(1 - d) \leq Q_{\max} \leq (1 + d)$), (2) if the stress constraints are not violated

(i.e., $R_{\max} \leq (1 + d)$, where R_{\max} is defined as before), and (3) if the optimality criterion is satisfied for the displacement constraints. Figures 10 and 11 show the results of the computed output.

Figure 10 shows the weight of the structure versus the number of critical designs. Note that the weight decreases under the displacement constraints. When after 42 cycles the stress constraints are added, the structural weight increases suddenly and then begins to decrease again until, at 44 cycles, the design becomes optimal. Figure 11 shows the thickness of selected elements versus the number of critical designs. In the final stages, when the design approaches the acceptable criteria, the thickness of the elements decreases, whereas at the intermediate stages it may increase or decrease. Figure 11 shows that, as expected, the elements closest to the central load elements have a greater thickness than the more distant elements that have achieved the minimum allowable thickness. The larger stresses are developed close to the central load elements.

4. CONCLUSIONS

The example problem demonstrates that optimal design of thin shells of arbitrary shape can be accomplished by a general-purpose synthesis program such as DESAP1. The major deficiency of the present algorithm is that it requires a large number of design cycles to reach convergence to the final design, which is typical of other structural optimization algorithms. The economy of computation could be improved considerably by using a uniform scaling operation.

Because the displacement-constraint design is based on the exact optimal criterion and thus has better convergence characteristics, it is important in running the program to use the displacement constraints first and then impose the stress constraints. Once the design has

converged under the displacement constraints, adding the stress constraints will result in only a few more design cycles.

If the design has stress constraints only, it is still worthwhile to impose contrived displacement constraints on the initial stages of the design procedure. These constraints should be replaced by the stress constraints after the initial design has converged.

5. ACKNOWLEDGMENTS

The author wishes to thank his former thesis advisor, Professor J. Kiusalaas, for his support. The work described herein was performed while the author was a graduate student in the Engineering Science and Mechanics Department at Pennsylvania State University, University Park, Pennsylvania.

APPENDIX — INVESTIGATION OF COEFFICIENTS C_{xx} and C
OF REDESIGN STRESS RATIO FORMULA

The stress ratio formula is a fourth-order equation in the variable $X = t'/t$, where t is the current thickness at the element and t' represents the improved thickness

$$X^4 - C_{xx}X^2 + C_xX - C = 0 \quad (11)$$

where the coefficient C_{xx} has the form

$$C_{xx} = (N_x/N_x^*)^2 + (N_y/N_y^*)^2 + (N_{xy}/N_{xy}^*)^2 - N_xN_y/N_x^*N_y^* \quad (10a)$$

where N_x , N_y , and N_{xy} are the normal and shear forces and N_x^* , N_y^* , and N_{xy}^* are the allowable normal and shear forces. Equation (10a) can be written as

$$C_{xx} = a^2 + b^2 + c^2 - ab$$

where $a = N_x/N_x^*$, $b = N_y/N_y^*$, and $c = N_{xy}/N_{xy}^*$. If ab is a nonpositive number (i.e., $ab \leq 0$), then C_{xx} is always a positive number. If ab is a nonnegative number (i.e., $ab \geq 0$), then

$$-ab \geq -2ab$$

Adding $a^2 + b^2 + c^2$ to both sides of this inequality gives

$$a^2 + b^2 + c^2 - ab \geq a^2 + b^2 + c^2 - 2ab$$

or

$$a^2 + b^2 + c^2 - ab \geq (a - b)^2 + c^2$$

Therefore,

$$a^2 + b^2 + c^2 - ab \geq 0$$

Consequently, C_{xx} is always a nonnegative real number if $ab \geq 0$.

The coefficient C of Eq. (11) has the form

$$C = (M_x/M_x^*) + (M_y/M_y^*)^2 + (M_{xy}/M_{xy}^*)^2 - (M_x/M_x^*)(M_y/M_y^*)$$

where M_x , M_y , and M_{xy} are the bending and twisting moments and M_x^* , M_y^* , and M_{xy}^* are the allowable bending and twisting moments as described previously. Again it can be shown that the coefficient C is always a nonnegative real number.

This reasoning was used for the analytical solution of Eq. (11).

REFERENCES

1. J. Kiusalaas, and G.B. Reddy, DESAP1—A Structural Design Program with Stress and Displacement Constraints. Vols. 1-3. NASA CR-2794 to 2796 (1977).
2. J. Kiusalaas and G.B. Reddy, DESAP2—A Structural Design Program with Stress and Bending Constraints. Vols. 1-3. NASA CR-2797 to 2799 (1977).
3. K. Wilkinson, et al., FASTOP: A flutter and strength optimization program for lifting-surface structures. *J. Aircraft*, **14**, 581-587 (1977).
4. V.P. Venkayya, Structural Optimization: A review and some recommendations. *Int. J. Numer. Methods Eng.*, **13**, 203-228 (1972).
5. K.J. Bathe, E.L. Wilson, and F.E. Peterson, SAPIV: A Structural Analysis Program for Static and Dynamic Response of Linear Systems. University of California, Berkeley, CA (1974).
6. J. Kiusalaas, Minimum Weight Design of Structures via Optimality Criteria. NASA TN D-7115, 31-41 (1972).
7. P.K. Gotsis, Optimization of Thin Shell Structures by the Finite Element Method. M.S. Thesis. Engineering Science and Mechanics Department, Pennsylvania State University, University Park, PA (1982).
8. O.C. Zienkiewicz, *The Finite Element Method*. Third ed. McGraw-Hill Book Company, New York, 335-337 (1977).
9. O.C. Zienkiewicz, C. Parekn, and I.P. King, Arch Dams Analysed by a Linear Finite Element Shell Solution. *Proc. Symp. Arch Dams*, Inst. Civil Eng., London, UK, 19-36 (1968).
10. S. Timosenko and S. Woinowsky-Krieger, *Theory of Plates and Shells*. McGraw-Hill Book Company, New York, 37-52 (1959).

11. L.W. Griffiths, *Introduction to The Theory of Equations*. John Wiley & Sons, Inc., New York, 33-42 (1947).
12. S. Borofsky, *Elementary Theory of Equations*. The Macmillan Company, New York, 115-130 (1961).
13. W. Flugge, *Stresses in Shells*. Springer-Verlag, New York (1973).
14. I. Holland, Fundamentals of the finite element method. *Comput. and Struct.*, 4, 3-15 (1974).
15. R.W. Clough and E.L. Wilson, Dynamic finite element analysis of arbitrary thin shells. *Int. J. Solids Struct.*, 7, 33-56 (1971).
16. R.W. Clough and C.P. Johnson, A finite element approximation for the analysis of thin shells. *Int. J. Solids Struct.*, 4, 43-60 (1968).
17. D. G. Aswell and R. H. Gallagher, *Finite Elements for Thin Shells and Curved Members*. John Wiley & Sons, New York, 245-263 (1974).

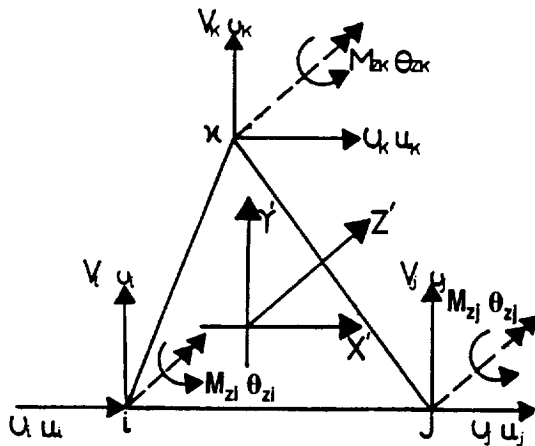


Figure 1.—In-plane forces and deformations in local system $X' Y' Z'$.

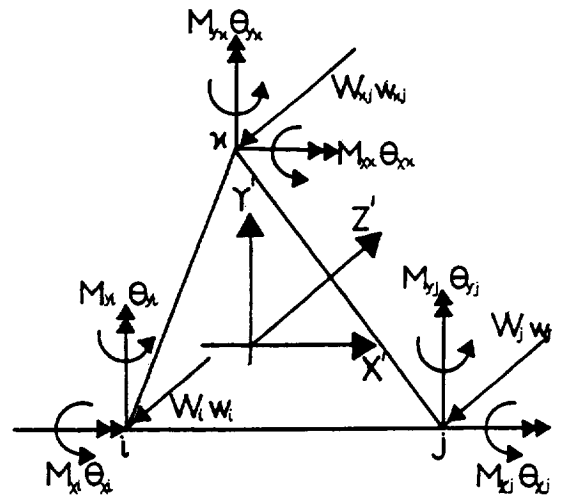


Figure 2.—Bending forces and deformations in local system $X' Y' Z'$.

U_i	V_i	W_i	Θ_{xi}	Θ_{yi}	Θ_{zi}	U_j	V_j	W_j	Θ_{xj}	Θ_{yj}	Θ_{zj}	U_k	V_k	W_k	Θ_{xk}	Θ_{yk}	Θ_{zk}
$k_{1,1}$	$k_{1,2}$					$k_{1,7}$	$k_{1,8}$					$k_{1,13}$	$k_{1,14}$				
$k_{2,1}$	$k_{2,2}$					$k_{2,7}$	$k_{2,8}$					$k_{2,13}$	$k_{2,14}$				
		$k_{3,3}$	$k_{3,4}$	$k_{3,5}$				$k_{3,9}$	$k_{3,10}$	$k_{3,11}$				$k_{3,15}$	$k_{3,16}$	$k_{3,17}$	
		$k_{4,3}$	$k_{4,4}$	$k_{4,5}$				$k_{4,9}$	$k_{4,10}$	$k_{4,11}$				$k_{4,15}$	$k_{4,16}$	$k_{4,17}$	
		$k_{5,3}$	$k_{5,4}$	$k_{5,5}$				$k_{5,9}$	$k_{5,10}$	$k_{5,11}$				$k_{5,15}$	$k_{5,16}$	$k_{5,17}$	
					B						C						C
$k_{7,1}$	$k_{7,2}$					$k_{7,7}$	$k_{7,8}$					$k_{7,13}$	$k_{7,14}$				
$k_{8,1}$	$k_{8,2}$					$k_{8,7}$	$k_{8,8}$					$k_{8,13}$	$k_{8,14}$				
		$k_{9,3}$	$k_{9,4}$	$k_{9,5}$				$k_{9,9}$	$k_{9,10}$	$k_{9,11}$				$k_{9,15}$	$k_{9,16}$	$k_{9,17}$	
		$k_{10,3}$	$k_{10,4}$	$k_{10,5}$				$k_{10,9}$	$k_{10,10}$	$k_{10,11}$				$k_{10,15}$	$k_{10,16}$	$k_{10,17}$	
		$k_{11,3}$	$k_{11,4}$	$k_{11,5}$				$k_{11,9}$	$k_{11,10}$	$k_{11,11}$				$k_{11,15}$	$k_{11,16}$	$k_{11,17}$	
					C						B						C
$k_{13,1}$	$k_{13,2}$					$k_{13,7}$	$k_{13,8}$					$k_{13,13}$	$k_{13,14}$				
$k_{14,1}$	$k_{14,2}$					$k_{14,7}$	$k_{14,8}$					$k_{14,13}$	$k_{14,14}$				
		$k_{15,3}$	$k_{15,4}$	$k_{15,5}$				$k_{15,9}$	$k_{15,10}$	$k_{15,11}$				$k_{15,15}$	$k_{15,16}$	$k_{15,17}$	
		$k_{16,3}$	$k_{16,4}$	$k_{16,5}$				$k_{16,9}$	$k_{16,10}$	$k_{16,11}$				$k_{16,15}$	$k_{16,16}$	$k_{16,17}$	
		$k_{17,3}$	$k_{17,4}$	$k_{17,5}$				$k_{17,9}$	$k_{17,10}$	$k_{17,11}$				$k_{17,15}$	$k_{17,16}$	$k_{17,17}$	
					C						C						B

Figure 3.—Stiffness matrix K and fictitious stiffness coefficients.

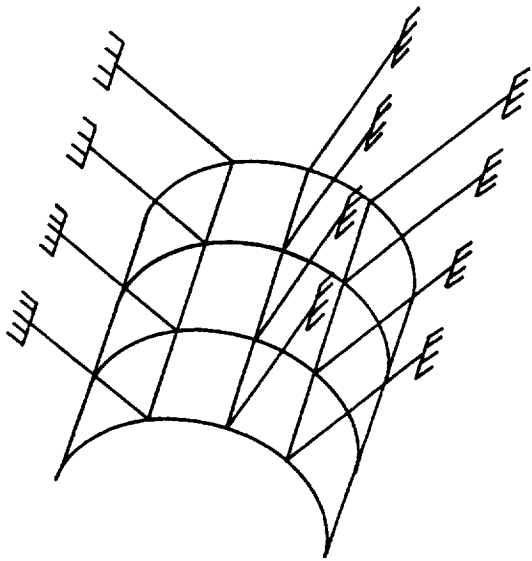


Figure 4.—Direction of boundary elements in typical shell structure.

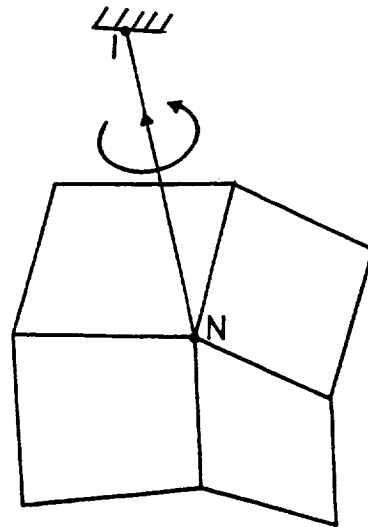


Figure 5.—First method of determining boundary elements.

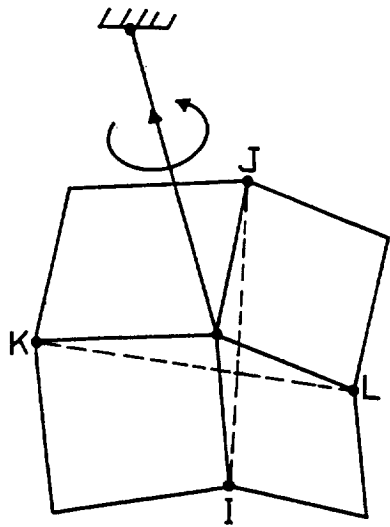


Figure 6.—Second method of determining boundary elements.

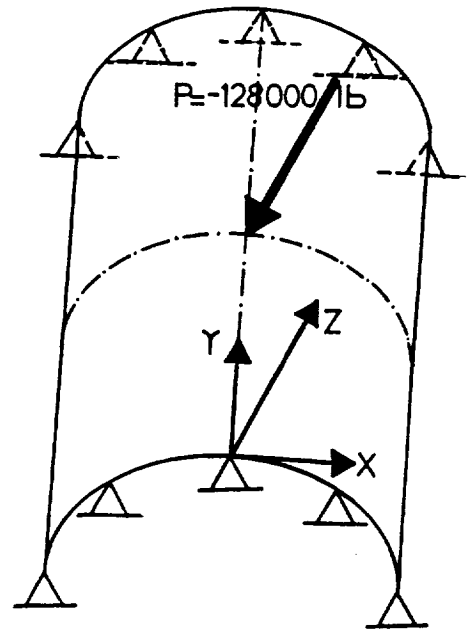


Figure 7.— Example of thin shell.

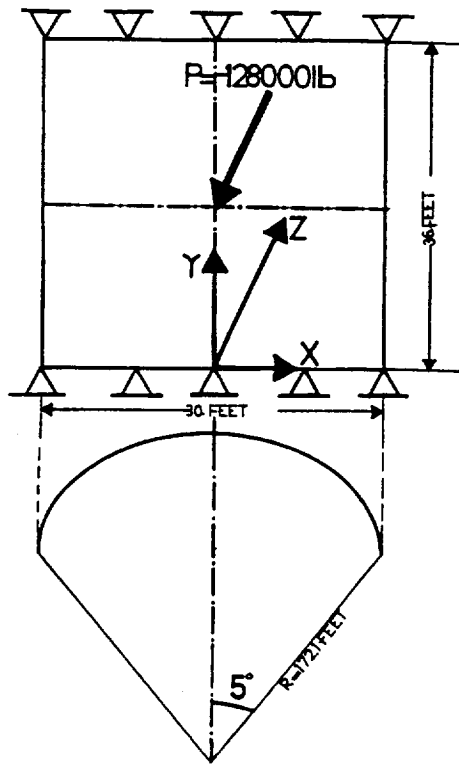


Figure 8.—Top view and cross-sectional area of thin shell.

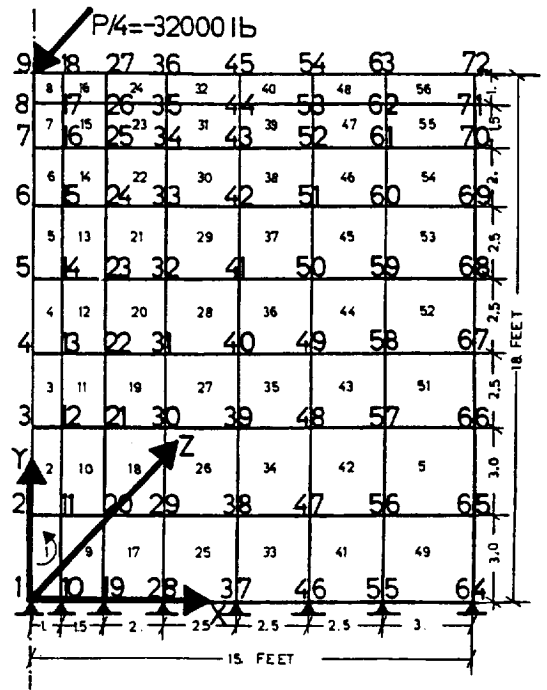


Figure 9.—Quarter section of thin shell to be modeled.

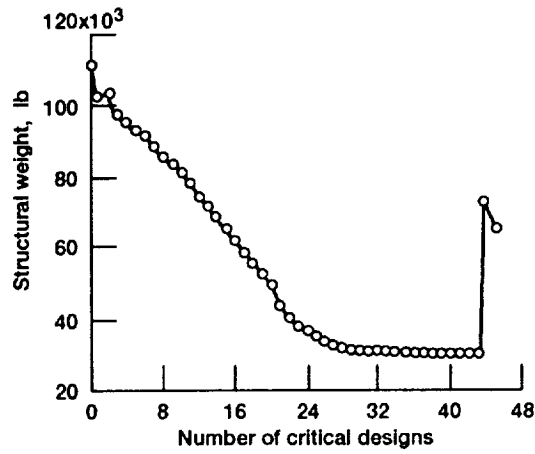


Figure 10.—Optimum design of thin, flat shell structure.

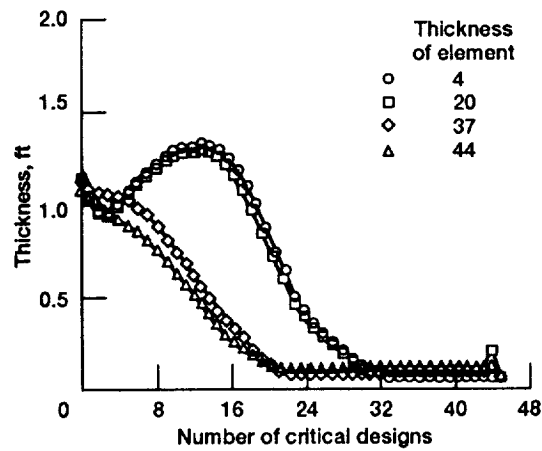


Figure 11.—Thickness of element versus number of designs.